ACADEMIA ROMÂNĂ
Revue Roumaine de Chimie
http://web.icf.ro/rrch/

Rev. Roum. Chim.,
2010, *55*(11-12), 755-763

Dedicated to the memory of
Professor Ioan Silaghi-Dumitrescu (1950–2009)

TEN-VERTEX CLUSTERS OF GERMANIUM, TIN AND LEAD CONTAINING INTERSTITIAL NICKEL, PALLADIUM AND PLATINUM ATOMS WITH 26 SKELETAL ELECTRONS: ISOVALENT ANALOGUES OF THE KNOWN $Pd@Bi_{10}^{4+}$**

R. Bruce KING,[a]* Ioan SILAGHI-DUMITRESCU[a,b]** and Matei-Maria UTA[b]

[a] Department of Chemistry, University of Georgia, Athens, Georgia, 30602
[b] Faculty of Chemistry and Chemical Engineering, Babeş-Bolyai University, Cluj-Napoca, Roumania

Received March 18, 2010

Structures for the metal-centered 26 skeletal electron 10-vertex tetrel clusters $M@Tt_{10}^{6-}$ (Tt = Ge, Sn, Pb) derived from polyhedra with 3-fold, 4-fold, and 5-fold symmetry have been studied by density functional theory. In the lowest energy $M@Ge_{10}^{6-}$ structures the Ge_{10} unit splits into two Ge_5 tetragonal pyramids, which are coordinated as trihapto ligands in $Ni@Ge_{10}^{6-}$, but as dihapto ligands in $Pd@Ge_{10}^{6-}$ and $Pt@Ge_{10}^{6-}$. A similar structure with dihapto tetragonal pyramid Ge_5 ligands is the lowest energy structure for $Pt@Sn_{10}^{6-}$. However, for $Pd@Sn_{10}^{6-}$ the lowest energy structure is an intact tetracapped trigonal prism. Structures with intact ten-vertex polyhedra are also the global minima for metal-centered clusters of the larger Pb_{10} polyhedra. However, these structures are different for all three metals. Thus the lowest energy structures for $M@Pb_{10}^{6-}$ are a distorted pentagonal prism, a tetracapped trigonal prism, and a pentagonal antiprism for the nickel, palladium, and platinum derivatives, respectively.

INTRODUCTION

Bare post-transition metal clusters were first observed by Zintl and co-workers[1-2] in the 1930s during studies of potentiometric titrations of the elements with alkali metals in liquid ammonia. Definitive structural characterization of such clusters was initially not feasible owing to difficulties in obtaining crystalline derivatives. However, finally in the 1960s Corbett and coworkers[3] found that complexation of alkali metal countercations with amines or cryptates led to crystalline derivatives of many of the anionic bare post-transition metal clusters suitable for structural characterization by X-ray crystallography. Corbett and co-workers[4] also characterized structurally a number of bare post-transition element cluster cations obtained in strongly Lewis acidic media.

The original post-transition element clusters were empty clusters containing no interstitial atoms in the centers of the cluster polyhedra. However, subsequent studies led to the discovery of clusters containing interstitial transition metals. The synthetic studies of Ruck[5] are of particular interest since they led to the discovery of extensive series of bismuth clusters containing interstitial transition metal atoms. Among the clusters discovered by Ruck, a particularly interesting metal-centered bismuth cluster is the pentagonal

* Corresponding author: rbking@chem.uga.edu
** This paper is dedicated to the memory of Prof. Ioan Silaghi-Dumitrescu (1950–2009) in recognition of his contributions to diverse areas of inorganic and computational chemistry as well as his leadership in Roumanian science.

antiprismatic $Pd@Bi_{10}^{4+}$ cation[6] found in the ternary halide $Bi_{14}PdBr_{10}$.

Initially the post-transition element clusters were assumed to be isoelectronic with the deltahedral boranes and related species. Thus bare vertices of the group 14 elements, such as germanium, tin, and lead, are considered to be isolobal and isoelectronic with the BH vertices found in deltahedral boranes. Similarly, bare vertices of the group 15 elements, such as arsenic, antimony, and bismuth, are considered to be isolobal and isoelectronic with the CH vertices found in deltahedral carboranes. Thus the Wade-Mingos rules,[7-10] which were originally developed to account for the structures and bonding in deltahedral boranes, were used initially to rationalize the structures and geometries of bare post-transition metal clusters. This method considers the $Pd@Bi_{10}^{4+}$ cation to be a 10-vertex arachno system with (2)(10) + 6 = 26 skeletal electrons (= $2n$ + 6 skeletal electrons for n = 10). This electron-counting scheme assumes that bare bismuth vertices each contribute 3 skeletal electrons leaving an "external" lone electron pair not involved in the skeletal bonding. The interstitial palladium atom is assumed to contribute zero skeletal electrons because of the stability of its filled d^{10} shell.[11] Such an arachno system with n vertices and $2n$ + 6 skeletal electrons is expected to have two non-triangular faces or one large open face with a shape derived from a deltahedron with n + 2 vertices by removing two of the vertices and all of the edges associated with them. The pentagonal antiprism is obviously derived in this way from an icosahedron by removing an antipodal pair of vertices leading to two pentagonal faces and D_{5d} point group symmetry.

For this reason the pentagonal antiprismatic structure of $Pd@Bi_{10}^{4+}$ initially did not appear to be particularly unusual. However, density functional theory (DFT) studies on bare germanium clusters in our group[12-18] indicated that for the 8, 11, and 14 vertex systems the favored deltahedra for the bare Ge_n^{2-} clusters are completely different from those of the corresponding deltahedral boranes (Figure 1). In these cases, the borane deltahedra have the maximum number of degree 5 vertices, where the degree of a vertex is the number of edges meeting at the vertex in question. However, the preferred deltahedra for the isovalent bare Ge_n^{2-} clusters were found to have only degree 4 and 6 vertices with no degree 5 vertices at all. This suggested that the Wade-Mingos rules[7-10] are not necessarily applicable to bare post-transition element clusters as had been previously believed. Instead the apparent "external" lone pairs in the bare post-transition element clusters are not truly external lone pairs but instead participate in the skeletal bonding.

These considerations led to the development of an alternative model[12] for the skeletal bonding in bare post-transition metal clusters based on the jellium model of physicists.[13,14] This model approximates the cluster by a sphere of negative charge arising from the electrons. This negative charge is counterbalanced by the positive charge of the nuclei forming the cluster in question. The resulting energy levels are based on spherical harmonics, somewhat analogous to atomic structure. In both cases "magic numbers" of systems of special stability relate to filled shells. For atomic structures where the positive charge is concentrated into a single concentrated nucleus at the center of the sphere, the magic numbers correspond to the noble gases, which exhibit exceptionally low chemical reactivities. However, for the jellium model[12] relating to cluster structures, the positive charges are distributed throughout the sphere leading to a different sequence of energy levels of the corresponding spherical harmonics. The "magic numbers" for special cluster stability are 20 and 40 total electrons. In this case, all of the valence electrons of the cluster atoms are counted, including the electrons considered to be "external" lone pairs for application of the Wade-Mingos rules.[7-10]

This jellium model accounts very well for the prevalence of 40 total valence electron clusters such as In_{11}^{7-} (ref. 15), $Ni@In_{10}^{10-}$ (ref. 16), and Ge_9^{4-} (refs. 17, 18, 19) as products from the synthesis of bare post-transition element clusters under forcing conditions, such as high temperature reactions.

Post-transition element cluster systems with ten vertices are of particular interest since stable structures have been found based on different ten-vertex polyhedra representing examples of three-fold, four-fold, and five-fold symmetry (Figure 2). Thus the isoelectronic systems $Ni@In_{10}^{10-}$ and $Zn@In_{10}^{8-}$ found in intermetallic structures were determined by X-ray crystallography to exhibit structures having 10-vertex deltahedra of different symmetries and topologies, namely the D_{4d} bicapped square antiprism for $Zn@In_{10}^{8-}$ (ref. 20) but a C_{3v} polyhedron for $Ni@In_{10}^{10-}$ (ref. 16). These experimental results are consistent with our theoretical results,[21] which, however, used the

isoelectronic germanium clusters $Ni@Ge_{10}$ and $Zn@Ge_{10}^{2+}$ to model the indium clusters to avoid the computational and other problems associated with the high negative charges on the indium clusters. Furthermore, for none of the related 26-skeletal electron 10-vertex germanium clusters in this study, namely $Ni@Ge_{10}^{6-}$, $Cu@Ge_{10}^{5-}$, and $Zn@Ge_{10}^{4-}$, was the pentagonal antiprism predicted to be the preferred structure.

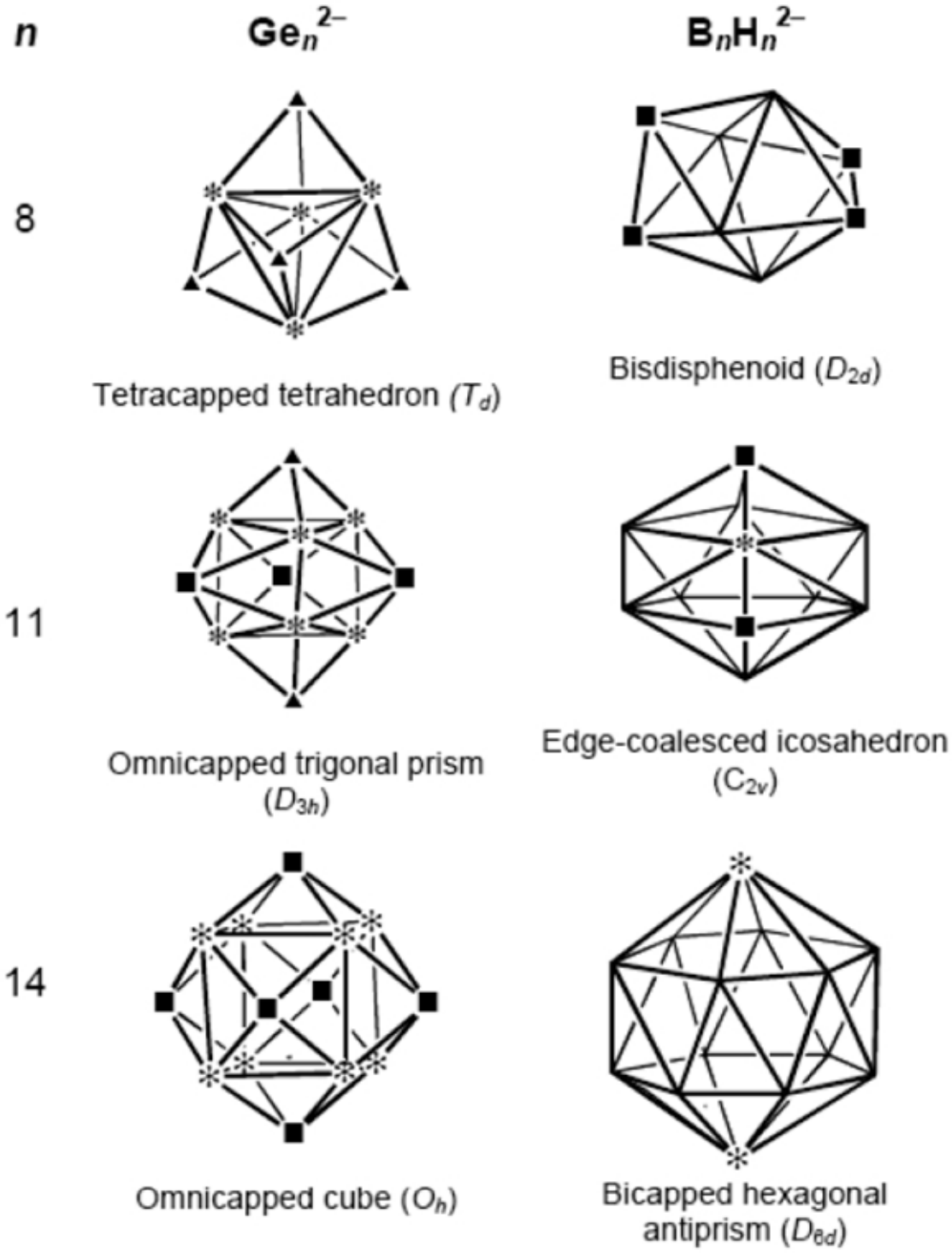

Fig. 1 – Examples of different lowest energy structures for isoelectronic Ge_n^{2-} and $B_nH_n^{2-}$ derivatives (n = 8, 11, 14). Degree 6, 4, and 3 vertices are indicated by ✻, ■, and ▲, respectively, and degree 5 vertices are unmarked.

The Wade-Mingos rules[7-10] predict cluster structures based on polyhedra in which all or most of the faces are triangles. For this reason the recent discovery (2009) of transition metal-centered 10-vertex germanium clusters based on the pentagonal prism with no triangular faces at all was a very provocative development indicating emphatically the inadequacy of the Wade-Mingos rules for rationalizing cluster structures. Both of these recently discovered pentagonal prismatic clusters are of the type $M@Ge_{10}^{3-}$ (M = Fe,[22] Co[23]), containing the transition metal in the center of the Ge_{10} pentagonal prism. With the discovery of these pentagonal prismatic clusters, all four of the 10-vertex polyhedra in Figure 2 have now been found in isolable bare metal clusters, which are sufficiently stable for structural characterization by X-ray diffraction.

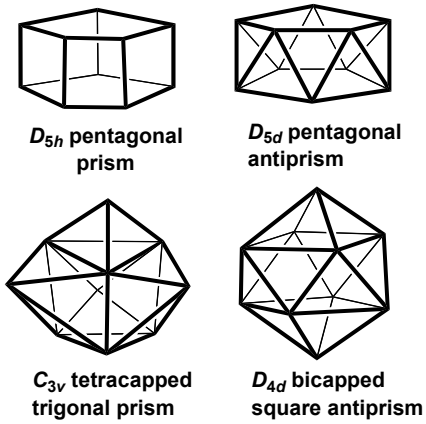

Fig. 2 – Ten-vertex polyhedra with three-, four-, and five-fold symmetry found in metal cluster structures.

Recently we used density functional theory to investigate the nine 26-skeletal electron systems $M@Pn_{10}^{4+}$ (M = Ni, Pd, Pt; Pn = As, Sb, Bi) in order to assess the relative stabilities of systems based on the different ten-vertex polyhedra (Figure 2).[24] The expected pentagonal antiprism from the Wade-Mingos rules,[7,8,9,10] was found to be the preferred structure for only the experimentally known $Pd@Bi_{10}^{4+}$ and the platinum analogue $Pt@Bi_{10}^{4+}$. The lowest energy polyhedral structures for the arsenic and antimony clusters $M@Pn_{10}^{4+}$ (Pn = As, Sb) and $Ni@Bi_{10}^{4+}$ are derived from a tetracapped trigonal prism.

This paper describes analogous theoretical studies on the isoelectronic 26-skeletal ten-vertex group 14 (tetrel) metal clusters $M@Tt_{10}^{6-}$ (M = Ni, Pd, Pt; Tt = Ge, Sn, Pb). The high negative charges on these systems frequently lead to splitting of the initial ten-vertex polyhedron into two smaller fragments during the optimization process. However, the pattern of splitting itself is of interest, suggesting new types of Ge_n ligands for transition metal chemistry.

COMPUTATIONAL METHODS

Geometry optimizations were carried out at the hybrid DFT B3LYP level[25-28] using ECP LANL2DZ basis sets with one additional f type polarization function for the interstitial atoms (Ni, Pd, Pt).[26] The ECP LANL2DZd basis sets[27] with one additional d polarization function were used for the tetrel cluster atoms (Ge, Sn, Pb). The Gaussian 03 package of programs[28] was used in which the fine grid (75,302) is the default for numerically evaluating the integrals and the tight (10^{-8}) hartree stands as default for the self-consistent field convergence. Computations were carried out using four initial geometries including ten-vertex polyhedra with three-fold, four-fold, and five-fold symmetry (Figure 2). The symmetries were maintained during the initial geometry optimization processes. Symmetry breaking using modes defined by imaginary vibrational frequencies was then used to determine the minimum energy optimized structures. Vibrational analyses show that all of the final optimized structures discussed in this paper are genuine minima at the B3LYP/LANL2DZ level without any significant imaginary frequencies. However, in a few cases the calculations ended with acceptable small imaginary frequencies[29] and these values are indicated in the corresponding figures.

The optimized structures found for the $M@Tt_{10}^{6-}$ clusters (M = Ni, Pd, Pt; Tt = Ge, Sn, Pb) (Figures 3, 4, and 5) are labeled by the central

metal atom (Ni, Pd, Pt) followed by the tetrel cluster atom (Ge, Sn, Pb). Since in several instances the initial symmetry was changed by following normal modes corresponding to imaginary vibrational frequencies, we do not use the point group symbol but instead indicate the order of the principal rotation axis of the starting structure. Furthermore **5** and **5*** are used to differentiate between the D_{5h} pentagonal prism and the D_{5d} pentagonal antiprism starting structures, respectively. Triplet structures are indicated by **T.** Thus the structure of $Ni@Ge_{10}^{6-}$, derived from a pentagonal antiprism starting structure, is labeled **NiGe-5***.

The structures considered in the text are limited to structures within 30 kcal/mol of the global minimum. Additional details of all of the optimized structures, including all interatomic distances and the initial geometries leading to a given optimized structure, are provided in the Supporting Information.

RESULS AND DISCUSSION

1. Germanium Clusters

None of the optimized lowest energy structures of the $M@Ge_{10}^{6-}$ derivatives (M = Ni, Pd, Pt) contains an intact ten-vertex polyhedron (Figure 3). Instead, in the lowest energy $M@Ge_{10}^{6-}$ structures the original Ge_{10} polyhedron splits into two identical Ge_5 fragments. These fragments are topologically similar to square pyramids, which are expected by the Wade-Mingos rules[7-10] to have 14 skeletal electrons and thus be Ge_5^{4-} tetranions. The central metal atoms in these $[M@(Ge_5)_2]^{6-}$ structures then exhibit the usual +2 formal oxidation states. The Ge_5^{4-} square pyramid ligands are distorted in the $M@Ge_{10}^{6-}$ structures where only two or three atoms of the pyramid base are bonded to the central metal atom. In these structures the base of the pyramid is not only not square but not even planar. Therefore these Ge_5^{4-} units are more accurately considered as tetragonal pyramids than ideal square pyramids.

In the lowest energy $Ni@Ge_{10}^{6-}$ structure **NiGe-5***, the Ge_5^{4-} tetragonal pyramids are bonded to the nickel atom (Figure 3) as trihapto ligands using three germanium atoms in the base of the pyramid. The tetragonal base of the tetragonal pyramid is distorted to non-planarity so that the basal germanium atom not bonded to the nickel moves away from the nickel atom to a distance of 3.902 Å. The Ni–Ge distances to the remaining three basal germanium atoms, are 2.60 ± 0.02 Å, which are clearly bonding distances. The two diagonals of the non-planar tetragonal base in **NiGe-5*** are 3.403 Å and 4.012 Å.

The shorter of these "non-bonding" diagonal Ge···Ge distances of 3.403 Å is clearly too long for the Ge_5 polyhedra in **NiGe-5*** to be considered as trigonal bipyramids rather than tetragonal pyramids. However, the distortion of the Ge_5 tetragonal pyramids for the trihapto bonding in **NiGe-5*** causes them to resemble trigonal bipyramids in Figure 3.

A higher energy triplet spin state $Ni@Ge_{10}^{6-}$ structure **NiGe-4T** (Figure 3) lies 8.1 kcal/mol above this global minimum **NiGe-5***. Structure **NiGe-4T** consists of two Ge_5Ni octahedra sharing the same nickel vertex. The highest energy $Ni@Ge_{10}^{6-}$ structure depicted in Figure 3 is **NiGe-5** at 20.3 kcal/mol above the **NiGe-5*** global minimum. The Ge_{10} network in structure **NiGe-5** appears to arise from partial opening of the pentagonal prism found in the starting structure from which **Ni-Ge5** is obtained.

The original Ge_{10} polyhedron also splits into two Ge_5^{4-} tetragonal pyramids in the lowest energy $M@Ge_{10}^{6-}$ (M = Pd, Pt) structures **PdGe-4** and **PtGe-4** (Figure 3). In these structures the central metal atom is coordinated to two diagonally opposite atoms of the tetragonal base of the Ge_5^{4-} pyramid as a bidentate (dihapto) chelating ligand. This leads to approximate square planar coordination, which is typical for these d^8 metals in the +2 oxidation state.

No other $Pd@Ge_{10}^{6-}$ structures were found within 30 kcal/mol of the global minimum **PdGe-4**. However, two higher energy $Pt@Ge_{10}^{6-}$ structures were found, namely **PtGe-3** and **PtGe-5*** at 16.7 and 25.5 kcal/mol, respectively, above the global minimum **PtGe-4** (Figure 3). In both of these structures the original Ge_{10} polyhedron splits into a Ge_4 and a Ge_6 unit. In **PtGe-3** both the Ge_6 and Ge_4 units function as trihapto ligands and the bonding details are similar to **NiGe-5*** with two trihapto Ge_5 ligands discussed above. In **PtGe-5** the Ge_6 ligand is a tetrahapto ligand derived from a bicapped tetrahedron and the Ge_4 ligand is a dihapto butterfly bonding to the platinum atom through its wingtips.

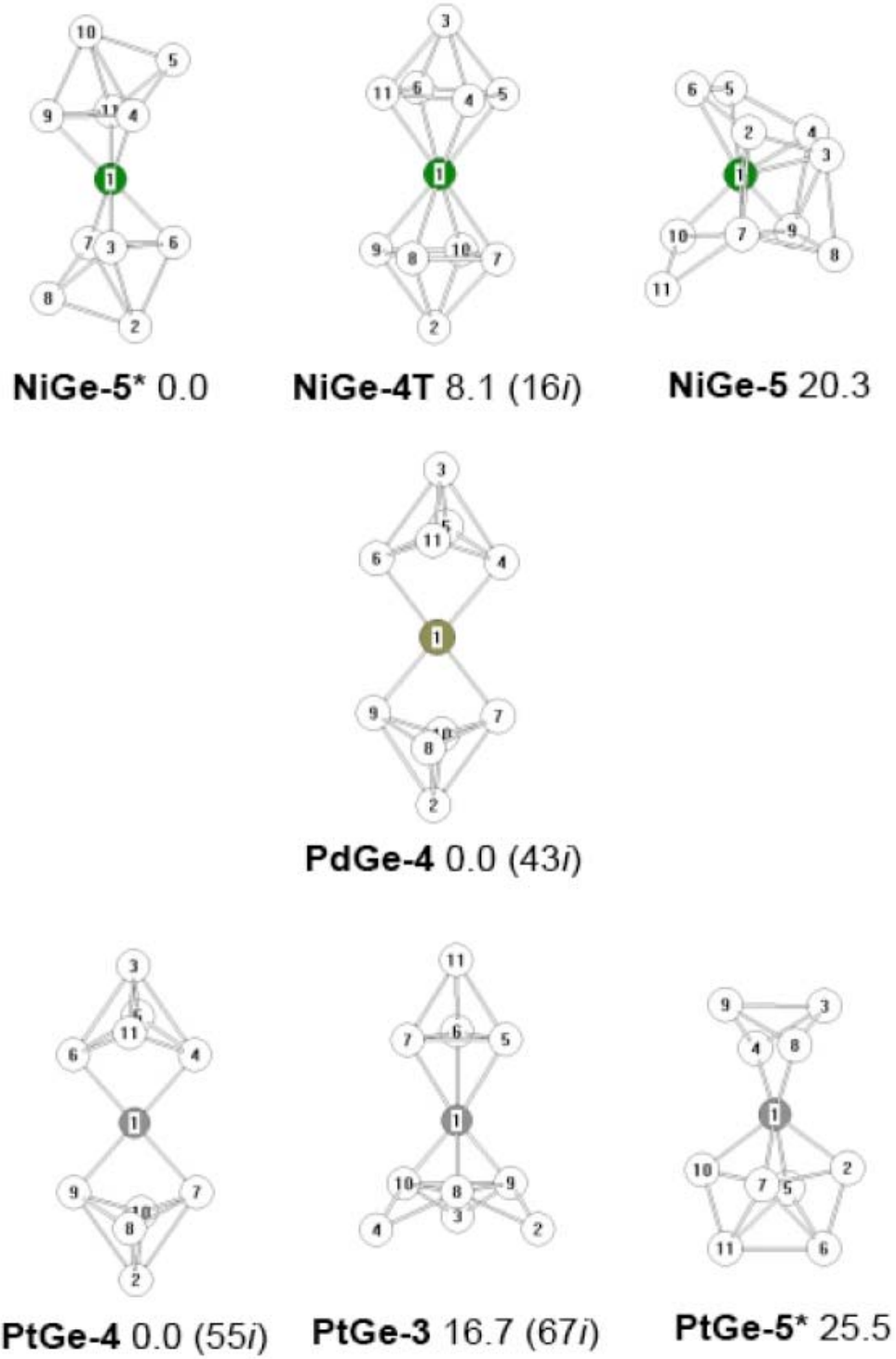

Fig. 3 – Structures of the $M@Ge_{10}^{6-}$ clusters (M = Ni, Pd, Pt) with relative energies in kcal/mol. Residual imaginary vibrational frequencies (in cm^{-1}) are shown in parentheses.

2. Tin Clusters

An intact tetracapped trigonal prism (Figure 4) is found for all three $M@Sn_{10}^{6-}$ clusters (M = Ni, Pd, Pt). For $Pd@Sn_{10}^{6-}$ this structure **(PdSn-3**) is the global minimum. However, for $Ni@Sn_{10}^{6-}$ and $Pt@Sn_{10}^{6-}$ the tetracapped trigonal prism structures **NiSn-3** and **PtSn-3** lie 12.9 kcal/mol and 22.9 kcal/mol, respectively, above the corresponding global minima. In all three cases these tetracapped trigonal prism structures were found to be the lowest energy $M@Sn_{10}^{6-}$ structures where the Sn_{10} polyhedra remain intact. This is in accord with the previous study[24] on the isoelectronic $M@Sb_{10}^{4+}$ derivatives where the tetracapped trigonal prismatic structures were found to be the lowest

energy structures in all three cases. However, the earlier study did not consider structures without intact Pn_{10} polyhedra (Pn = As, Sb, Bi), except for $M@As_{10}^{4+}$ (M = Pd, Pt), where no genuine minima with intact Pn_{10} polyhedra were found.

In the global minima for the two $M@Sn_{10}^{6-}$ systems (M = Ni, Pt) the original Sn_{10} polyhedron has split into two Sn_5 fragments. The global minimum for $Ni@Sn_{10}^{6-}$, namely **NiSn-4T** (Figure 4), is a triplet spin state structure similar to the $Ni@Ge_{10}^{6-}$ structure **NiGe-4T** (Figure 3), consisting of two Sn_5Ni octahedra sharing the nickel vertex. Similarly, the global minimum for **PtSn-4** (Figure 4) is essentially the same as that for **PtGe-4** (Figure 3) with two distorted square pyramidal Sn_5^{4-} clusters functioning as bidentate ligands towards the Pt(II) atom, thereby leading to square planar platinum coordination.

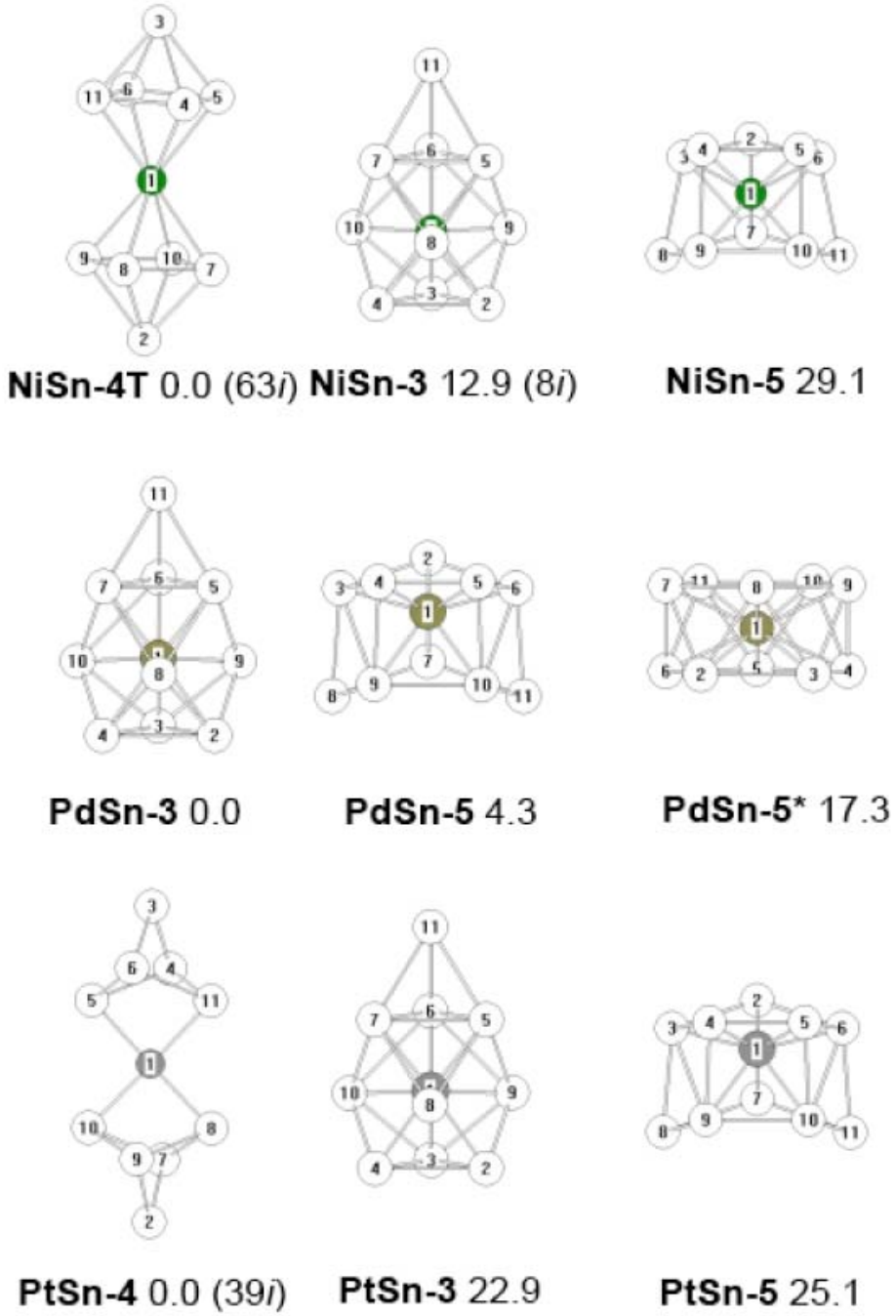

Fig. 4 – Structures of the $M@Sn_{10}^{6-}$ clusters (M = Ni, Pd, Pt) with relative energies in kcal/mol. Residual imaginary vibrational frequencies (in cm^{-1}) are indicated in parentheses.

Higher energy structures were found for all three $M@Sn_{10}^{6-}$ clusters (M = Ni, Pd, Pt) based on a distorted Ge_{10} pentagonal prism, namely structures **NiSn-5**, **PdSn-5**, and **PtSn-5** at 29.1, 4.3, and 25.1 kcal/mol above the corresponding global minima (Figure 4). Similar distorted pentagonal prism structures were found for the corresponding $M@Pn_{10}^{4+}$ clusters, also never as the global minima.[24] In addition, a higher energy pentagonal antiprism structure **PdSn-5*** (Figure 4) was found at 17.3 kcal/mol above the global minimum **PdSn-3**.

3. Lead Clusters

The pentagonal antiprism structures suggested by the Wade-Mingos rules[7,8,9,10] were found for all three $M@Pb_{10}^{6-}$ clusters (Figure 5). For **PtPb-5*** such a structure is the global minimum. The corresponding pentagonal antiprism structures **NiPb-5*** and **PdPb-5*** are predicted to have energies of 8.3 and 21.6 kcal/mol, respectively, above the corresponding global minima. The global minimum of $Ni@Pb_{10}^{6-}$, namely **NiPb-5** (Figure 5), is a distorted pentagonal prism similar to **NiSn-5**, **PdSn-5**, and **PtSn-5** (Figure 4). The global minimum of $Pd@Pb_{10}^{6-}$, namely **PdPb-3** (Figure 5), is a tetracapped trigonal prism similar to **PdSn-3**. Other higher energy $M@Pb_{10}^{6-}$ structures include the pentagonal prism structures **NiPb-5** and **PtPb-5** at 20.8 and 15.3 kcal/mol, respectively, above the corresponding global minima, the triplet spin state bicapped square antiprism structure **PtPb-4T** at 26.0 kcal/mol above **PtPb-5***, and an irregular polyhedral structure **PdPb-4** at 20.1 kcal/mol above **PtPb-3** (Figure 5).

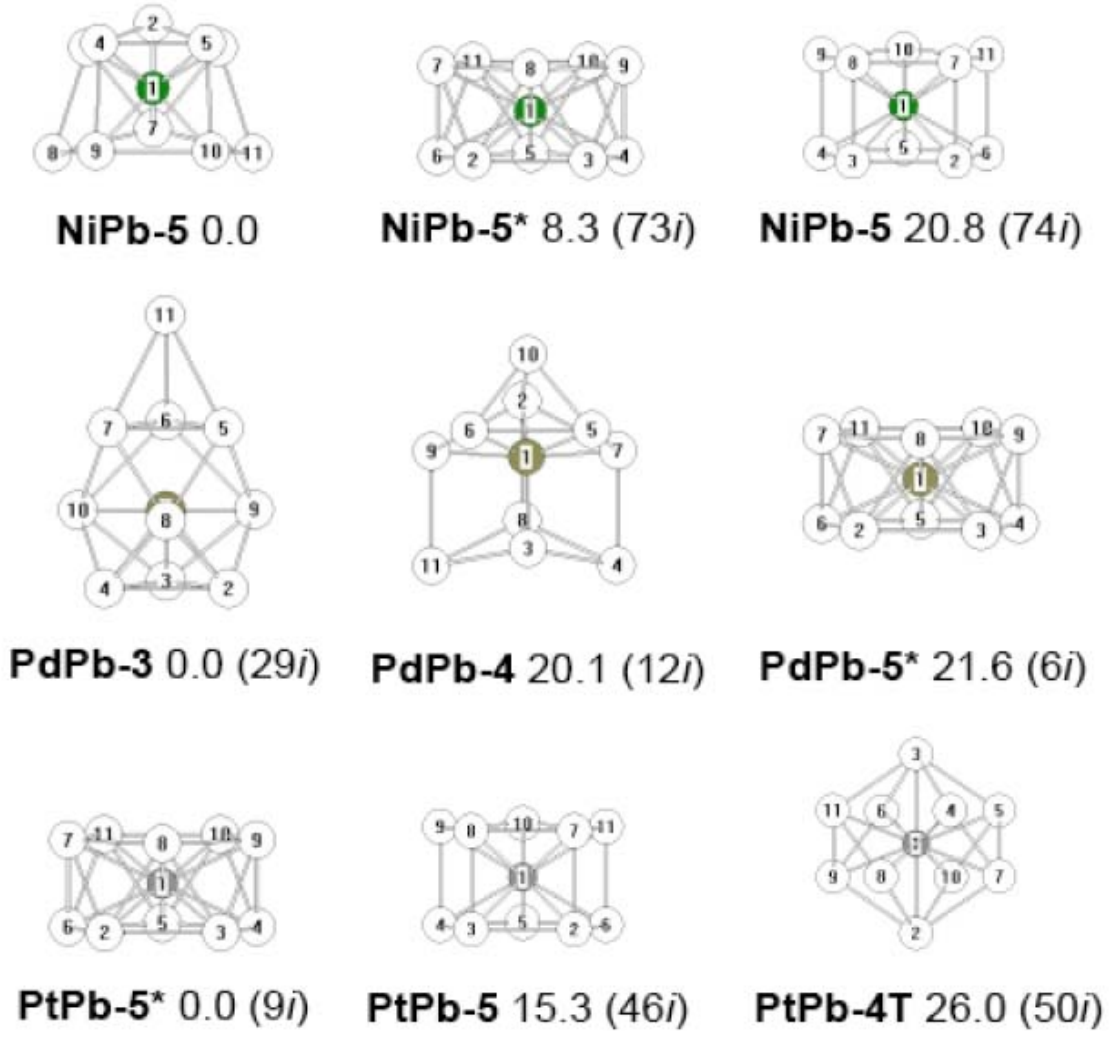

Fig. 5 – Structures of the $M@Pb_{10}^{6-}$ clusters (M = Ni, Pd, Pt) with relative energies in kcal/mol. Residual imaginary vibrational frequencies (in cm^{-1}) are indicated in parentheses.

CONCLUSION

In many of the lowest energy $M@Tt_{10}^{6-}$ (Tt = Ge, Sn, Pb) structures the ten-vertex polyhedron splits into two smaller fragments. This is particularly true for $M@Ge_{10}^{6-}$, because of the smaller cavity in the Ge_{10} polyhedron relative to the larger Sn_{10} and Pb_{10} polyhedra. Thus in the lowest energy structures for $M@Ge_{10}^{6-}$ the Ge_{10} unit splits into two tetragonal pyramids, which, according to the Wade-Mingos rules,[7,8,9,10] are Ge_5^{4-} tetraanions leading to the usual metal +2 formal oxidation states. The Ge_5^{4-} tetragonal pyramids are trihapto ligands in $Ni@Ge_{10}^{6-}$ but only dihapto ligands in $Pd@Ge_{10}^{6-}$ and $Pt@Ge_{10}^{6-}$. A related structure is the lowest energy structure for $Pt@Sn_{10}^{6-}$.

In contrast to the $M@Ge_{10}^{6-}$ structures, the larger 10-vertex tin and lead polyhedra remain intact in the $M@Sn_{10}^{6-}$ and $M@Pb_{10}^{6-}$ structures. Thus, for $Pd@Sn_{10}^{6-}$ the lowest energy structure is an intact tetracapped trigonal prism. Different structures, all with intact 10-vertex polyhedra, are found for the interstitial lead clusters $M@Pb_{10}^{6-}$. Thus the lowest energy structures for $M@Pb_{10}^{6-}$ are a distorted pentagonal prism, a tetracapped trigonal prism, and a pentagonal antiprism for the nickel, palladium, and platinum derivatives, respectively.

Acknowledgment: We are indebted to the National Science Foundation for support of this work under Grant CHE-0716718. Part of this work was undertaken with financial support from the CMMCCC 130/2007 program, Roumania.

Supporting Information Available (see http://web.icf.ro/rrch/)**:** Table S1. $Ni@Ge_{10}^{6-}$ optimized structures; Table S2. $Pd@Ge_{10}^{6-}$ optimized structures; Table S3. $Pt@Ge_{10}^{6-}$ optimized structures; Table S4. $Ni@Sn_{10}^{6-}$ optimized structures; Table S5. $Pd@Sn_{10}^{6-}$ optimized structures; Table S6. $Pt@Sn_{10}^{6-}$ optimized structures; Table S7. $Ni@Pb_{10}^{6-}$ optimized structures; Table S8. $Pd@Pb_{10}^{6-}$ optimized structures; Table S9. $Pt@Pb_{10}^{6-}$ optimized structures; Complete Gaussian03 reference (reference 28)

REFERENCES

1. E. Zintl, J. Goubeau and W. Dullenkopf, *Z. Phys. Chem., Abt. A*, **1931**, *154*, 1.
2. E. Zintl and Kaiser, H. *Z. Anorg. Allgem. Chem.,* **1933**, *211*, 113.
3. J. D. Corbett, *Chem. Rev.*,**1985**, *85*, 383.
4. J. D. Corbett, *Prog. Inorg. Chem.,* **1976**, *21*, 129.
5. M. Ruck, *Angew. Chem. Int. Ed.,* **2001**, *40*, 1182.
6. M. Ruck, V. Dubenskyy and T. Söhnel, *Angew. Chem. Int. Ed.,* **2003**, *42*, 2978.
7. K. Wade, *Chem. Comm.*, **1971**, 792.
8. K. Wade, *Adv. Inorg. Chem. Radiochem*., **1976**, *18*, 1.
9. D. M. P. Mingos, *Accts. Chem. Res*., **1984**, *17*, 311.
10. D. M. P. Mingos, R. L. Johnston, *Structure and Bonding,* **1987**, *68*, 29.
11. R. B. King, *Dalton Trans,*. **2004**, 3420.
12. R. B. King and I. Silaghi-Dumitrescu, *Dalton Trans.,* **2008**, 6083.
13. W. A. De Heer, *Rev. Mod. Phys.,* **1993**, *65*, 611.
14. E. Janssens, S. Neukermans and P. Lievens, *Current Opinion in Solid State and Materials Science*, **2004**, *8*, 185.
15. S. C. Sevov and J. D. Corbett, *Inorg. Chem.,* **1991**, *30*, 4877.
16. R. W. Henning and J. D. Corbett, *Inorg. Chem.*, **1999**, *38*, 3883.
17. T. F. Fässler, *Coord. Chem. Revs.*, **2001**, *215*, 347.
18. V. Quéneau, E. Todorov and S. C. Sevov, *J. Am. Chem. Soc.*, **1998**, *120*, 3263.
19. H. G. von Schnering, M. Somer, M. Kaupp, W. Carillo-Cabrera, M. Basitinger, A. Schmeding and Y. Grin, *Angew. Chem. Int. Ed.*, **1998**, *37*, 2359.
20. S. C. Sevov and J. C. Corbett, *Inorg. Chem.,* **1993**, *32*, 1059.
21. R. B. King, I. Silaghi-Dumitrescu and M.-M. UTA, *Chem. Eur. J.,* **2008**, *14*, 4542
22. B. Zhou, M. S. Denning, D. L. Kays and J. M. Goicoechea, *J. Am. Chem.Soc.,* **2009**, *132*, 2802.
23. J.-Q. Wang, S. Stegmaier and T. F. Fässler, *Angew Chem. Int. Ed.,* **2009**, *48*, 1998.
24. R. B. King, I. Silaghi-Dumitrescu and M.-M. UTA, *Inorg. Chem.*, **2009**, *48*, 8508.
25. S. H. Vosko, L. Wilk and M. Nusair, *Can. J. Phys*., **1980**, *58*, 1200.
26. L. E. Roy, P. J. Hay and R. L. Martin, *J. Chem. Theory Comput*., **2008**, 4, 1029.
27. C. E. Check, T. O. Faust, J. M. Bailey, B. J. Wright, T. M. Gilbert and L. S. Sunderlin, *J. Phys. Chem. A,* **2001**, *105*, 8111.
28. M. J. Frisch *et al.,* Gaussian 03, Revision C 02; Gaussian, Inc.; Wallingford CT, 2004 (see Supporting Information for details; http://web.icf.ro/rrch/).
29. Y. Xie, H. F. Schaefer III and R. B. King, *J. Am. Chem. Soc*., **2000**, *122*, 8746.